



# Parametric Study on the Influence of Embedded SPR to the Performance of Square CFST Columns

Abdul Azim Abdullah<sup>1,2\*</sup>, Azrul Abdul Mutalib<sup>2\*</sup>, Shahrizan Baharom<sup>2</sup>, Wan Hamidon Wan Badaruzzaman<sup>2</sup>

<sup>1</sup>Department of Civil Engineering,  
Universiti Malaysia Sarawak, 94300 Kota Samarahan, MALAYSIA

<sup>2</sup>Department of Civil Engineering,  
Universiti Kebangsaan Malaysia, 43600 Bangi, MALAYSIA

\*Corresponding Author

DOI: <https://doi.org/10.30880/ijie.2020.12.09.023>

Received 27 August 2020; Accepted 24 November 2020; Available online 30 December 2020

**Abstract:** Steel plate reinforcements (SPR) embedded into the concrete core of a concrete filled steel tube (CFST) column is a promising strengthening scheme. However, further study is required to understand the influence SPR on the strength and behaviour of a CFST column. Numerical models of the CFST columns are developed using finite element analysis. The models are verified with experimental results from past research. The models are in good agreement with the experimental study. Then, a parametric study is conducted to investigate the strength and behaviour of CFST columns embedded with various configuration of SPR. In which, the embedded SPR varies in quantity, thickness and height. The parametric study indicates that these factors have positive influence on the performance of the CFST columns. The performance of the columns is measured in terms of strength, stiffness and ductility. Results have shown that the performance of the columns increases with every increment of the quantity, thickness and height of SPR.

**Keywords:** CFST, columns, embedded steel plate reinforcements, finite element analysis, strengthening scheme

## 1. Introduction

Concrete filled steel tube (CFST) columns with circular cross-section have better structural performance compared to square section. It is well known that circular steel tubes provide high confining stress to its concrete core. In contrast, the confining stress distribution of a square CFST sections is non-uniform, hence less confinement. Moreover, the axial strength of a square CFST columns are further reduced when the depth-to-thickness ratio are high due to local buckling [1]–[3]. However, the square CFST members are more preferable due to its high moment capacities, easy beam-to-column connections and aesthetic consideration. Researchers have proposed different type of strengthening scheme to improve its strength.

Utilization of longitudinal plate stiffener is a well-known method in improving the resistance of a square CFST column. Longitudinal plate stiffeners are welded on the inner surface of the steel tubes. Experimental tests [3]–[6] have shown that the longitudinal stiffeners can delay local buckling, improves the confinement pressure on the concrete core and thus increasing the resistance and ductility of the CFST columns. The ultimate load of a square CFST columns with one longitudinal stiffener on each steel tube surface was reported to be around 10% higher than unstiffened sections [7], [8].

An interesting way of attaching inner longitudinal stiffeners was demonstrated in [9]. In which, the inner longitudinal stiffeners were intermittently welded to the inner surface of the steel tube through the predrilled holes. The strength and stiffness of CFST columns were influenced by the spacing of the weld and quantity of the stiffener plates. Ghanim [10] investigate on the mechanical performances of CFST columns stiffened using reinforcing bars (RB) welded to the inner tube. Twenty-two CFST columns were tested to determine the effect of utilizing different diameters, quantity and patterns of RB. It was found that the strength, ductility and stiffness of CFST columns increasing as the number of RBs increased.

All the strengthening scheme as discussed were able to improve the mechanical properties of the square CFST columns. However, the existing stiffeners may have limitations in construction practice, for example, longitudinal plate stiffeners need to be welded to the steel tube and the welding process if not done carefully will introduce unnecessary residual stresses and imperfections. Abdullah [11] investigate the possibility of embedding longitudinal steel plate into the concrete core of a square CFST column instead of welding it to the steel tube. Typical cross-section of a square CFST column with embedded SPR is shown in Fig. 1. The embedded steel plate reinforcements (SPR) were able to improve the performance of the column. However, further investigation is required to understand the influence of SPR. Hence, a parametric study is conducted to determine the effect of quantity, height and thickness of the embedded SPR.

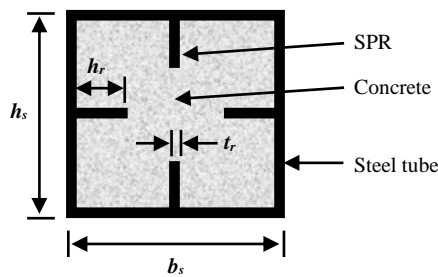


Fig. 1 - Typical cross-section of CFST column with SPR

Nomenclature	
$b_s$	width of the steel tube
$f_{b0}$	biaxial compressive strength
$f_c^*$	uniaxial compressive strength
$h_r$	height of SPR
$h_s$	height of the steel tube
$K_c$	ratio of the second stress invariant on the tensile meridian to that on the compressive meridian
$K_e$	stiffness
$M$	moment
$N$	axial load
$N_{max}$	ultimate load
$t_r$	thickness of SPR
$t_s$	thickness of the steel tube
$u$	mid-height deflection
$\Delta_c$	deflection at maximum load
$\Delta_{max}$	maximum deflection
$\Delta_y$	yield deflection
$\epsilon$	strain
$\epsilon_{cr}$	critical tensile strain
$\epsilon_t$	tensile strain
$\mu$	ductility
$\rho_s$	reinforcement ratio
$\sigma$	stress
$\sigma_t$	tensile stress
$\sigma_{t0}$	maximum tensile stress
$\psi$	dilation angle
$\epsilon$	flow potential eccentricity

## 2. Numerical Model

This section will outline on the development of the 3D finite element method (FEM) models. Finite element software named ABAQUS was used in this study. In order to develop an accurate model, careful selection of the material properties for steel and confined concrete, interaction between steel tube and concrete, type of element, mesh size and also boundary conditions are essential. Four-node shell elements with reduced integration (S4R) was used to model the steel tube. As for the concrete core, it is modelled using eight-node continuum elements with reduced integration (C3D8R). Optimal mesh size was determined by conducting mesh convergence study. The element size across the cross-section was chosen equal to  $B/14$ , where  $B$  is the width or height of the steel tube. The total number of elements are more than 20000.

The bottom boundary condition is fully restraint except for the in-plane rotation. Similar boundary conditions are imposed at top of the column except for the vertical displacement at the loaded end. Load is applied at the top of the column through vertical displacements. Explicit dynamic analysis was used to perform quasi-static analysis. The primary advantage of using this method is that it can find solutions up to failure especially when brittle materials such as concrete in tension and large number of contact points between steel tube and concrete core are involved. Additionally, the solution cost for the explicit procedure rises linearly with problem size, whereas for implicit procedure the solution cost rises exponentially with problem size. However, check on the kinetic energy of the column is required so that it is very small compared to the internal energy. This is to ensure that the problem remains static.

## 3. Material Model

### 3.1 Steel

The elastic-perfectly plastic model was used to represent the constitutive behaviour of steel. Steel does not exhibit significant strain hardening at general structural interest strains of less than 5%. The steel tube of a square CFST member is susceptible to local buckling and provide less effective confinement to the concrete core. Hence, the type of stress-strain relationship has negligible influence on the ultimate strength and only affects the load-deformation curve slightly in the later stage. Steel yield stress and elastic modulus used in the model are similar to the one used in [11]. The Poisson ratio is taken as 0.3.

### 3.2 Concrete

The concrete damage plasticity (CDP) model available in ABAQUS was used to model the triaxial behaviour of the confined concrete core. Tensile cracking and compressive crushing of concrete are the main failure mechanism in this model. The stress-strain behaviour of concrete in uniaxial compression was used to define concrete behaviour in compression. The three-stage stress-strain curve proposed by Tao [12], shown in Fig. 2, was adopted to describe the uniaxial compressive behaviour of the concrete. The CDP model incorporates nonassociated potential plastic flow. The behaviour of the flow potential is a function of the dilation angle ( $\psi$ ) and flow potential eccentricity ( $\epsilon$ ). For rectangular columns the dilation angle of  $40^\circ$  can be used [12].

The flow potential eccentricity determines the rate at which the function approaches the asymptote. The default flow potential eccentricity, equal to 0.1, was used. The parameters involved in defining the yield function are the ratio of the second stress invariant on the tensile meridian to that on the compressive meridian ( $K_c$ ) and ratio of biaxial compressive strength to uniaxial compressive strength ( $f_{b0}/f_c'$ ). The default value of  $2/3$  and  $1.16$  were used respectively. The Poisson ratio of the concrete was taken equal to 0.2. The concrete cracking behaviour in tension was modelled using the tension stiffening model proposed by Wahalathantri [13] (Fig. 3). In this model, the two descending portions of the tensile stress-strain behaviour were able to capture the concrete response caused by primary and secondary cracking phenomena.

## 4. Contact Interaction and Constraint

The contact interaction at the steel tube and concrete core interface was modelled in the normal and tangential directions. The interaction in the normal direction was defined using hard contact pressure-overclosure relationship. In this interaction, the concrete core is allowed to separate from the steel tube in tension and the concrete core cannot penetrate the steel tube in compression. While the interaction in the tangential direction, the penalty friction formulation was used with coulomb friction coefficient taken as 0.60 [12] and the interfacial shear stress limit is equal to 0.41 MPa [14]. The steel plate reinforcements were modelled using the embedded region constraint. In which, the SPR were defined as the embedded region within the concrete core as the host.

## 5. Model Verification

The FEM models developed in this study were verified against the experimental test conducted in [11]. Fig. 4 shows the comparison on the load-deflection response between the models and test specimens. As a result, a very good agreement can be seen between the models and test specimens. The models were able to capture the response of the CFST columns embedded with SPR. The ultimate load for column A and B measured from experimental test were

281.91 kN and 317.72 kN respectively. While the predicted ultimate load is 281.17 kN for column A and 308.35 kN for column B.

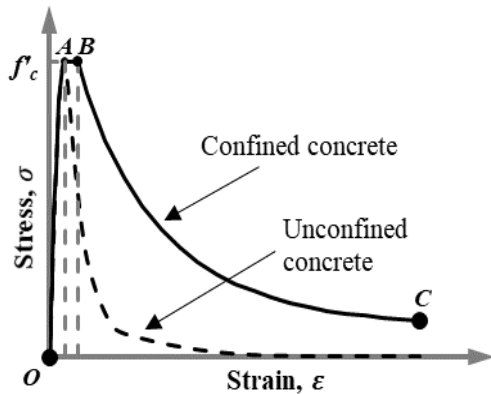


Fig. 2 - Concrete model in compression

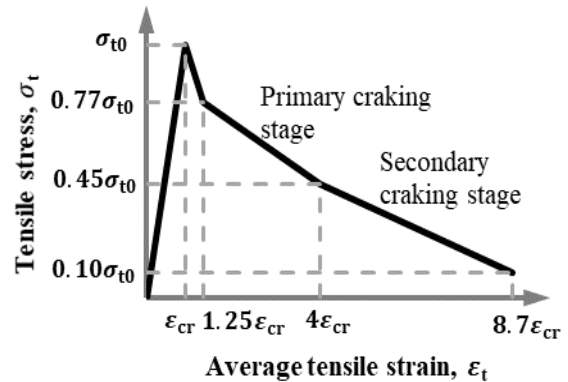


Fig. 3 - Concrete model in tension

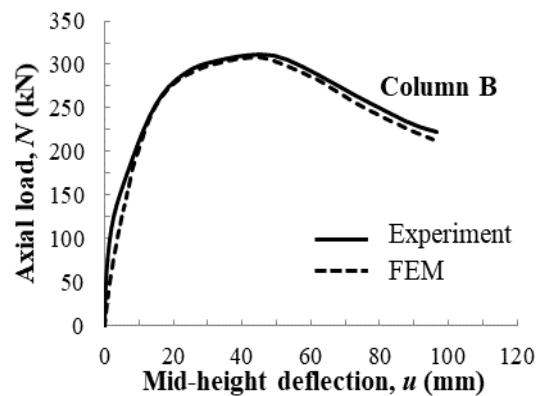
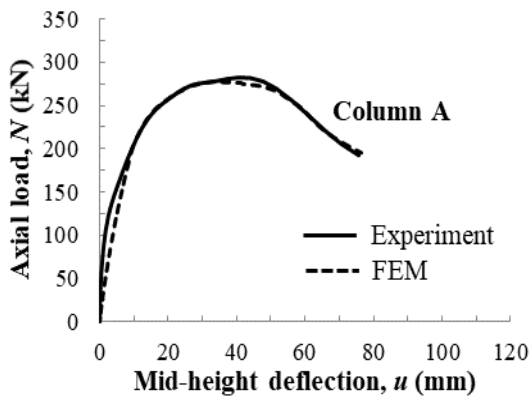


Fig. 4 - Comparison on the load-deflection response between experiment and FEM

## 6. Parametric Study

In this section, investigation is done to determine the effect of using SPR in terms strength, stiffness and ductility of CFST columns. The SPR adopted in the following section will be differ in quantity, thickness and height. The cross-section of the steel tube considered in this parametric study is 200 mm x 200 mm x 4.5 mm ( $b_s \times h_s \times t_s$ ) and 3 m in height. The yield strength for the steel tube is chosen as 300 MPa, while its modulus of elasticity is 205 GPa. Similar yield strength and modulus of elasticity are adopted for SPR. The reinforcement ratio  $\rho_s$ , area of SPR over area of concrete, is 0 to 4.65%. The boundary conditions are roller and pin, at the top and bottom of the column respectively. The concrete strength  $f_c'$  is 35 MPa. All column considered in the parametric studies hereafter have the same attributes as stated above unless stated otherwise.

### 6.1 SPR Quantity

The effect of quantity of SPR provided on each side of the steel tube's inner wall is studied in this section. The columns considered here are C0, C1, C2 and C3. The cross-sections of the columns and detail of the SPR dimensions can be found in Fig. 5. Column without SPR (C0) would be the benchmark to how much improvement can be gain by increasing quantity of SPR. The height and thickness of SPR are similar for all column, 30 mm and 4.5 mm respectively. Fig. 6 shows the load-displacement response for these columns. It can be seen that the addition of SPR does improve the ultimate strength of CFST columns. The ultimate strength increases as the number of SPR increases. The improvement in strength, stiffness and ductility can be seen in Table 1. Ductility,  $\mu$  is defined as the division of the maximum deflection,  $\Delta_{max}$  over the yield deflection,  $\Delta_y$  [7]. The  $\Delta_y$  is defined by the secant stiffness connecting the origin and 75% ultimate load. While, the  $\Delta_{max}$  is defined as the post ultimate load deflection corresponding to 85% of the ultimate strength. The N-M diagram of the columns is shown in Fig. 7. The axial capacity for all columns decreases with increase in moment. Columns with embedded SPR possess higher compression and moment resistance.

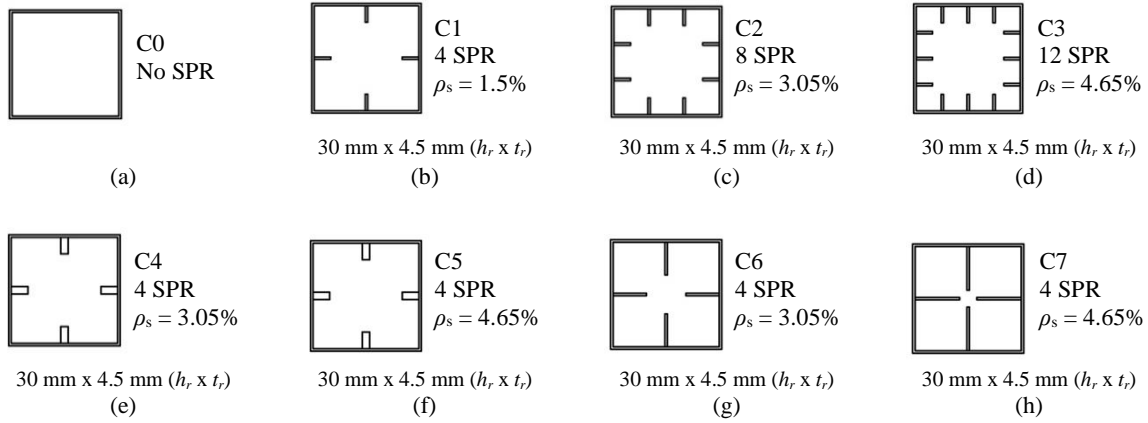


Fig. 5 - Cross-sections and SPR configurations used in the parametric study

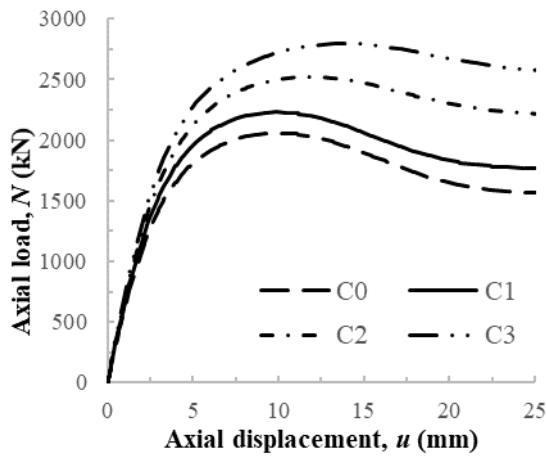


Fig. 6 - Load-displacement comparison between C0, C1, C2 and C3

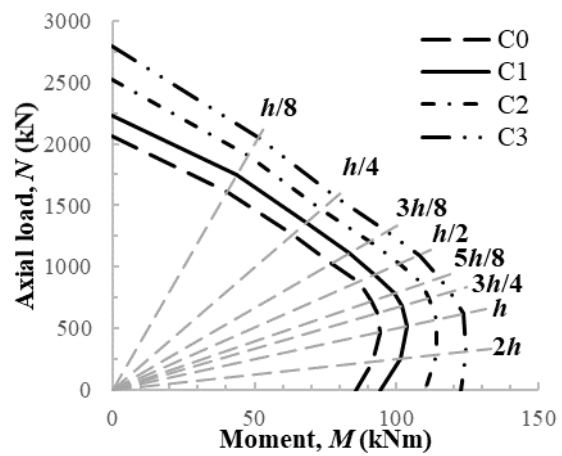


Fig. 7 - N-M diagram comparison between C0, C1, C2 and C3

Table 1 - Stiffness, strength and ductility of column C0, C1, C2 and C3

Column	Stiffness			Strength			Ductility		
	$\Delta_y$ (mm)	$K_e$ (kN/mm)	Improve ment	$\Delta_c$ (mm)	$N_{max}$ (kN)	Improve ment	$\Delta_{max}$ (mm)	$\mu$	Improve ment
C0	4.61	447	-	9.83	2058	-	4.63	1.01	-
C1	4.66	478	7%	9.85	2231	8%	18.20	3.90	288%
C2	5.15	490	10%	11.80	2523	23%	38.87	7.55	652%
C3	5.54	505	13%	13.93	2795	36%	36.75	6.64	560%

### 6.2 SPR Thickness

The effect of varying SPR thickness with regard to the strength, stiffness and ductility of CFST column are presented here. Column C1, C5 and C6 shown in Fig. 5 are considered. All columns are embedded with one SPR per side. The thickness of SPR varies from 4.5 mm, 9 mm to 13.5 mm. The height of SPR is fixed at 30 mm for all thickness. The load-displacement response for these columns are plotted in Fig. 8. The load carrying capacity of the CFST column increases with each increment of the SPR thickness. Comparison on the strength, stiffness and ductility can be seen in Table 2. Furthermore, CFST columns embedded with thicker SPR have higher compression and moment resistance as shown in Fig. 9. Columns with thicker SPR perform better when the eccentricity is applied beyond the column face.

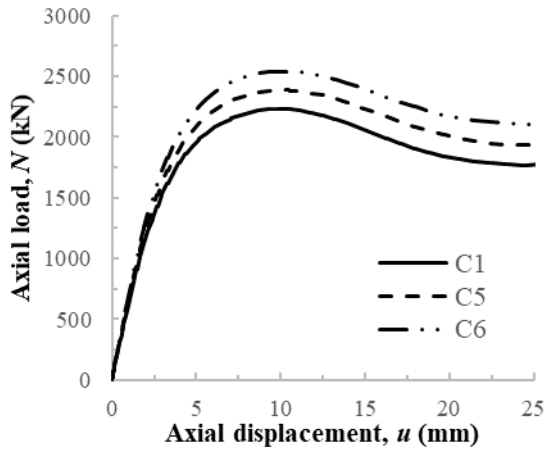


Fig. 8 - Load-displacement comparison between C1, C5 and C6

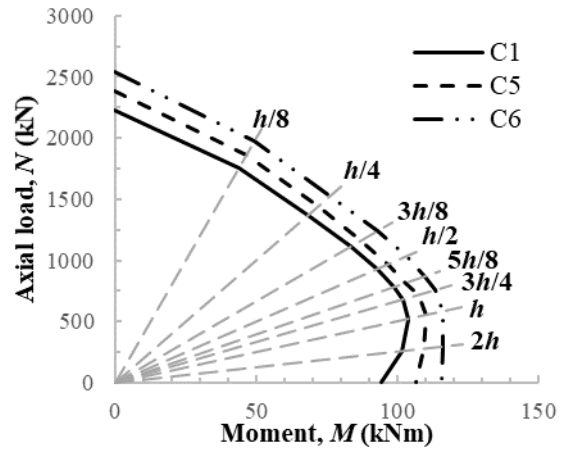


Fig. 9 - N-M diagram comparison between C1, C5 and C6

Table 2 - Stiffness, strength and ductility of column C1, C5 and C6

Column	Stiffness			Strength			Ductility		
	$\Delta_y$ (mm)	$K_e$ (kN/mm)	Improve ment	$\Delta_c$ (mm)	$N_{max}$ (kN)	Improve ment	$\Delta_{max}$ (mm)	$\mu$	Improve ment
C1	4.66	478	-	9.85	2231	-	18.20	3.90	-
C5	4.69	509	6%	9.85	2386	7%	19.38	4.13	6%
C6	4.73	538	12%	9.86	2542	14%	20.46	4.33	11%

### 6.3 SPR Height

The height of the SPR is another parameter which potentially could influence the strength and behaviour of the CFST columns. Column C1, C8 and C9 are considered in this comparison. All columns are embedded with one SPR per side but varies in height (Fig. 5). The height of SPR is selected to be 30 mm, 60 mm and 90 mm. The thickness of SPR remain unchanged at 4.5 mm for all SPR height. Increase in SPR height has positive influence on the strength, stiffness and ductility of the column as shown in Fig. 10 and Table 3. The ultimate load increases with increase in SPR height. Similar to the other parameters, columns with taller SPR have higher compression and moment resistance (Fig. 11). Columns with taller SPR have higher moment resistance when higher eccentricity was applied.

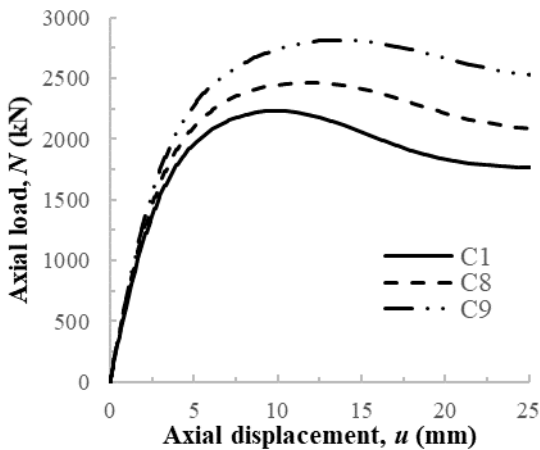


Fig. 10 - Load-displacement comparison between C1, C8 and C9

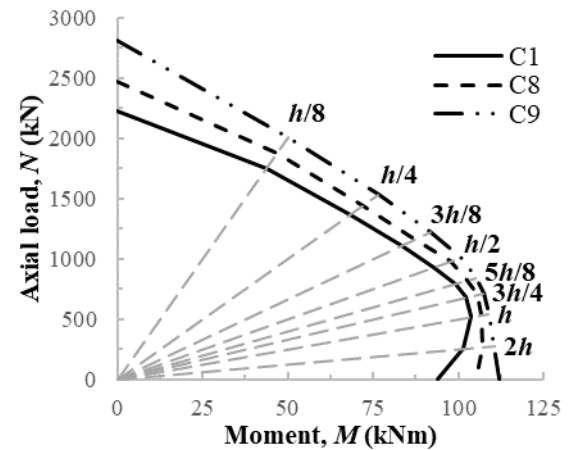


Fig. 11 - N-M diagram comparison between C1, C8 and C9

**Table 3 - Stiffness, strength and ductility of column C1, C8 and C9**

Column	Stiffness			Strength			Ductility		
	$\Delta_y$ (mm)	$K_e$ (kN/mm)	Improve ment	$\Delta_c$ (mm)	$N_{max}$ (kN)	Improve ment	$\Delta_{max}$ (mm)	$\mu$	Improve ment
C1	4.66	478	-	9.85	2231	-	18.20	3.90	-
C8	4.96	497	4%	11.79	2466	11%	24.16	4.87	25%
C9	5.61	502	5%	13.92	2816	26%	38.66	6.89	77%

## 7. Concluding Remarks

A quasi-static 3D numerical model has been developed and verified against experimental results obtain from [11]. Parametric study was conducted based on the numerical model to investigate the influence of SPR on the strength and behaviour of a CFST column. The parametric study focuses on the influence of the quantity, thickness and height of SPR on the performance of the square CFST columns. It was found that increasing one of these factors definitely have positive influence on the strength, stiffness and ductility of the column. The strength of the column embedded with SPR is 8% higher than the one without SPR. Further increase in strength can be observed in each increment of SPR quantity, 23% and 36% of improvement for 8 and 12 numbers of SPR respectively. Significant improvement in ductility can be seen for CFST column with embedded SPR. Average improvement of 7% in terms of strength, stiffness and ductility can be expected with every increment of the thickness of SPR. As for the height of SPR, 11% and 26% of improvement in strength when the height of SPR were increased from 30 mm to 60 mm and 90 mm respectively. Overall, the number of SPR is the best parameter to increase the strength and ductility of a CFST column subjected axial compression. Then, followed by the height and thickness of SPR. As for the column stiffness, the thickness of SPR is most influential followed by its height and quantity. Lastly, the N-M interaction diagrams show that columns with SPR were able to resist higher moment due to eccentricity in comparison with the one without SPR. The compression and moment resistance of a CFST column with SPR increases with increase in the quantity, thickness and height of SPR.

## Acknowledgement

The authors wish to acknowledge the financial supports from Universiti Malaysia Sarawak under research grant F02-SpMYRA-1718-2018.

## References

- [1] Bridge, R. Q. and O'Shea, M. D. (1998). Behaviour of thin-walled steel box sections with or without internal restraint. *J. Constr. Steel Res.*, 47, 73–91.
- [2] Han, L-H, Yao, G. H. and Zhao, X. L. (2005). Tests and calculations of hollow structural steel (HSS) stub columns filled with self-consolidating concrete (SCC). *J. Constr. Steel Res.*, 61, 1241–69.
- [3] Tao, Z., Han, L. and Wang, Z. (2005). Experimental behaviour of stiffened concrete-filled thin-walled hollow steel structural ( HSS ) stub columns. *J. Constr. Steel Res.*, 61, 962–83.
- [4] Tao, Z., Han, L. and Wang, D. (2007). Experimental behaviour of concrete-filled stiffened thin-walled steel tubular columns. *Thin-Walled Struct.*, 45, 517–27.
- [5] Zhu, A., Zhu, H., Zhang, X. and Lu, Y. (2016). Experimental study and analysis of inner-stiffened cold-formed SHS steel stub columns. *Thin-Walled Struct.*, 107, 28–38.
- [6] Zhu, A., Zhang, X., Zhu, H., Zhu, J. and Lu, Y. (2017). Experimental study of concrete filled cold-formed steel tubular stub columns. *J. Constr. Steel Res.*, 134, 17–27.
- [7] Lee, H., Choi, I. and Park, H. (2016). Eccentric Compression Strength of Rectangular Concrete-Filled Tubular Columns Using High-Strength Steel Thin Plates. *J. Struct. Eng.*, 143, 1–11.
- [8] Yuan, F., Huang, H. and Chen, M. (2019). Effect of stiffeners on the eccentric compression behaviour of square concrete-filled steel tubular columns. *Thin-Walled Struct.*, 135, 196–209.
- [9] Thomas, J. and Sandeep, T. N. (2020). Capacity of short circular CFST columns with inner vertical plates welded intermittently. *J. Constr. Steel Res.*, 165, 105840.
- [10] Ghanim, H., Ekmekyapar, T. and Shehab, B. A. (2019). Mechanical performances of stiffened and reinforced concrete- filled steel tubes under axial compression. *Mar. Struct.*, 65, 417–32.
- [11] Abdullah, A. A., Abdul Mutalib, A., Baharom, S. and Wan Badaruzzaman, W. H. (2018). Mechanical Behavior of Square CFST Columns with Embedded Steel Plate Reinforcement. *Int. J. Struct. Civ. Eng. Res.*, 7, 319–22.
- [12] Tao, Z. (2014). Refined finite element modelling of concrete- filled steel stub columns Proceedings of The Australasian Structural Engineering 2014 Conference (ASEC 2014) (Auckland, New Zealand).
- [13] Wahalathantri, B. L., Thambiratnam, D. P., Chan, T. H. and Fawzia, S. (2011). A material model for flexural

crack simulation in reinforced concrete elements using ABAQUS Proceedings of the First International Conference on Engineering, Designing and Developing the Built Environment for Sustainable Wellbeing (Brisbane, Qld), 260–264

- [14] Lai, Z., Varma, A. H. and Griffis, L. G. (2015). Analysis and Design of Noncompact and Slender CFT Beam-Columns. *J. Struct. Eng.*, 142, 04015097.